Anal. Chem. **2009,** *81,* 991–999

Three-Dimensional in Situ Temperature Measurement in Microsystems Using Brownian Motion of Nanoparticles

Kwanghun Chung, Jae Kyu Cho, Edward S. Park, Victor Breedveld, and Hang Lu*

School of Chemical & Biomolecular Engineering, Georgia Institute of Technology, Atlanta, Georgia 30332

We report an in situ method for three-dimensionally resolved temperature measurement in microsystems. The temperature of the surrounding fluid is correlated from Brownian diffusion of suspended nanoparticles. We use video-microscopy in combination with image analysis software to selectively track nanoparticles in the focal plane. This method is superior with regards to reproducibility and reduced systematic errors since measuring Brownian diffusivity does not rely on fluorescence intensity or lifetime of fluorophores. The efficacy of the method is demonstrated by measuring spatial temperature profiles in various microfluidic devices that generate temperature gradients and by comparing these results with numerical simulations. We show that the method is accurate and can be used to extract spatial temperature variations in three dimensions. Compared to conventional methods that require expensive multiphoton optical sectioning setups, this technique is simple and inexpensive. In addition, we demonstrate the capability of this method as an in situ tool for simultaneously observing live cells under the microscope and monitoring the local temperature of the cell medium without biochemical interference, which is crucial for quantitative studies of cells in microfluidic devices.

Recent developments in microsystems for chemical and biological analysis offer significant advantages over conventional methods, such as precise manipulation of samples and control of microenvironment.[1−4] For many applications, the ability to control and measure temperature inside microfluidic devices is critical since temperature often affects biological or chemical processes.[5−11] For instance, precise temperature control over time and/or space is essential for on-chip amplification of DNA sequences by Polymerase Chain Reaction (PCR).[8] In another case, a strong temperature-dependence and stringent regulations of the embryonic development of *Drosophila melanogaster* was demonstrated using a microfluidic device that generates a temperature differential across the embryos.[7] Besides controlling biological processes, temperature also plays a role in device functions. Numerous studies have demonstrated the importance of temperature effects in capillary electrophoresis systems.[6,9−11] For instance, temperature gradients in electrophoresis capillaries have long been understood to cause band spreading that reduces separation efficiency.[11] Thus, a reliable on-chip temperature measurement method is essential to design and operate microsystems effectively.

To address this need, many temperature measurement methods in microsystems have been developed. The common solution is to use microfabricated thermocouples for temperature measurement in microfluidic devices.[12−14] However, this approach constrains the measurements to specific fixed positions in the microdevices. As an alternative to microfabricated thermocouples, spectroscopic methods can provide temperature measurements with submicron spatial resolution by taking advantage of the temperature dependence of material properties of chemicals.[15−21] For example, thermochromic liquid crystals (TLC) have been successfully used as thermal probes,[19,22] but the high viscosity of TLCs limits their applications.[19] Fluorescent dyes are another class of commonly used thermosensitive chemicals. Rhodamine-B, for example, has been broadly used because high spatial- and temporal-resolution can be achieved with fluorescence microscopy.[18] However, these measurements are based on the magnitude of fluorescence intensity, which can often be affected by environmental factors, such as uneven illumination from the light source, adsorption of Rhodamine-B on polymer-based microfluidic

* To whom correspondence should be addressed. E-mail: hang.lu@gatech.edu. Phone: 1-404-894-8473. Fax: 1-404-894-4200.

(1) Vilkner, T.; Janasek, D.; Manz, A. *Anal. Chem.* **2004**, *76*, 3373–3385.
(2) Whitesides, G. M. *Nature* **2006**, *442*, 368–373.
(3) Dittrich, P. S.; Tachikawa, K.; Manz, A. *Anal. Chem.* **2006**, *78*, 3887–3907.
(4) deMello, A. J. *Nature* **2006**, *442*, 394–402.
(5) Chung, K. H.; Crane, M. M.; Lu, H. *Nat. Methods* **2008**, *5*, 637–643.
(6) Cao, J.; Hong, F. J.; Cheng, P. *Int. Commun. Heat Mass Transfer* **2007**, *34*, 1048–1055.
(7) Lucchetta, E. M.; Lee, J. H.; Fu, L. A.; Patel, N. H.; Ismagilov, R. F. *Nature* **2005**, *434*, 1134–1138.
(8) DeMello, A. J. *Nature* **2003**, *422*, 28–29.
(9) Ross, D.; Locascio, L. E. *Anal. Chem.* **2002**, *74*, 2556–2564.
(10) Rush, R. S.; Cohen, A. S.; Karger, B. L. *Anal. Chem.* **1991**, *63*, 1346–1350.
(11) Gobie, W. A.; Ivory, C. F. *J. Chromatogr. A* **1990**, *516*, 191–210.
(12) Pearce, T. M.; Wilson, J. A.; Oakes, S. G.; Chiu, S. Y.; Williams, J. C. *Lab Chip* **2005**, *5*, 97–101.
(13) Arata, H. F.; Rondelez, Y.; Noji, H.; Fujita, H. *Anal. Chem.* **2005**, *77*, 4810–4814.
(14) Yamamoto, T.; Nojima, T.; Fujii, T. *Lab Chip* **2002**, *2*, 197–202.
(15) Filevich, O.; Etchenique, R. *Anal. Chem.* **2006**, *78*, 7499–7503.
(16) Dowling, K.; Hyde, S. C. W.; Dainty, J. C.; French, P. M. W.; Hares, J. D. *Opt. Commun.* **1997**, *135*, 27–31.
(17) Samy, R.; Glawdel, T.; Ren, C. L. *Anal. Chem.* **2008**, *80*, 369–375.
(18) Ross, D.; Gaitan, M.; Locascio, L. E. *Anal. Chem.* **2001**, *73*, 4117–4123.
(19) Stasiek, J. A.; Kowalewski, T. A. *Opto-Electron. Rev.* **2002**, *10*, 1–10.
(20) Benninger, R. K. P.; Koc, Y.; Hofmann, O.; Requejo-Isidro, J.; Neil, M. A. A.; French, P. M. W.; deMello, A. *J. Anal. Chem.* **2006**, *78*, 2272–2278.
(21) Jeon, S. M.; Turner, J.; Granick, S. *J. Am. Chem. Soc.* **2003**, *125*, 9908–9909.
(22) Hoang, V. N.; Kaigala, G. V.; Backhouse, C. J. *Lab Chip* **2008**, *8*, 484–487.

10.1021/ac802031j CCC: $40.75
Published on Web 12/30/2008

chip material, and photobleaching.[17] In particular, variations in excitation and detection efficiencies across the microscope field of view can hinder quantitative interpretation of the intensity data, making these dyes unsuitable for accurate temperature measurement without complicated calibration. To overcome some of the shortcomings of the intensity-based temperature measurement, ratiometric fluorescence techniques and fluorescence lifetime imaging can be made since the readout signal is independent of intensity.[20,21] However, these techniques are often associated with specialized and expensive equipment.

Another important drawback of these conventional techniques is that the addition of the probes could perturb device function,[17,23] or be potentially toxic to biological samples.[24,25] It has been reported that organic small-molecule fluorescent dyes commonly used for temperature measurement can adsorb onto and diffuse into walls of polymer microfluidic chips.[17,23,26] In some instances, the adsorption of the charged dyes may alter surface chemistry of the microchannels, which results in unpredictable operation of electroosmotically pumped flow and electrophoretic separations.[17,23] Chemical probes have also been reported to be toxic to biological samples.[24,25] For example, Rhodamine-B inhibits the proliferation of human lip fibroblasts significantly, even at concentrations lower than that generally used for temperature measurements.[25]

The adsorption and toxicity of the thermosensitive chemicals can sometimes be addressed by separating the probes from the samples.[17,19] One approach is by using a thin PDMS membrane saturated with Rhodamine-B dye and sandwiching it between two glass substrates, thereby allowing temperature measurement in the presence of biological samples.[17] However, such temperature measurements are indirect because of the non-negligible thickness of the dye film and the glass substrate. Encapsulated beads of thermochromic liquid crystals also can be used for temperature measurements without altering the sample system.[19] The main drawback is that the encapsulated beads are typically tens of micrometers in size and are therefore impractical for use in micrometer-sized channel structures. As a result, in most studies that apply these methods, temperature profiles in microfluidic devices have been characterized without the actual devices in operation or without the presence of biological samples.

However, the presence of samples and the operation of integrated functional components can actually generate local temperature changes.[27,28] For example, it was found that the position and orientation of a *Drosophila* embryo affects the temperature distribution in a microfluidic device that was designed to generate temperature differential around the embryo.[27] In another example, dielectrophoretic cell separation causes Joule heating around electrodes and thus increases the local temperature, especially along the vertical dimension, which can lead to hyperthermic cell damage.[28] Therefore, to optimize the design and the operation of microsystems effectively, it would be desirable to characterize temperature while the device is in operation without introducing artifacts to the measurements or toxicity to the samples.

To address this need, we present in this work a novel three-dimensional (3-D) in situ temperature measurement method using the Brownian motion of nanoparticles with a simple and inexpensive videomicroscopy setup. This technique takes advantage of the well-defined temperature dependence of the Brownian motion of nanoparticles,[29,30] and offers several benefits over existing methodologies. First, tracking the Brownian motion of nanoparticles is independent of fluorophore intensity; therefore, it is superior in reproducibility and has reduced systematic error. Second, three-dimensionally resolved temperature measurements can be achieved without using an expensive multiple-photon scanning setup. Lastly, tracer particles can be selected or modified to be chemically inert and non-toxic to biological samples and therefore can be used for in situ temperature measurement during device operation.

EXPERIMENTAL METHOD AND MATERIALS

Fabrication of Polydimethylsiloxane (PDMS) Devices. The microfluidic devices were fabricated using multilayer soft lithography.[31] Negative molds were fabricated by UV photolithographic processes using a negative photoresist (SU8-2050, Microchem, Newton, MA). Patterned wafers were then treated with tridecafluoro-1,1,2,2-tetrahydrooctyl-1-trichlorosilane vapor (United Chemical Technologies, Bristol, PA) in a vacuum desiccator to prevent adhesion of PDMS (Sylgard 184, Dow Corning, Midland, MI) before the molding process. For all PDMS fabrication processes, a PDMS mixture of A and B in 5:1 ratio was used to minimize deformation of the PDMS structures while in device operation. For single-layer devices, a PDMS mixture was poured onto the mold to obtain a 5 mm thick layer and then fully cured at 70 °C for 2 h. In the case of two-layer devices, a PDMS mixture was spin-coated on the sample channel mold to give a 100 μm-thick layer, which resulted in a 30 μm-thick PDMS membrane on top of the sample channel. The same ratio of PDMS was poured onto the wafer mold for temperature-control channels to obtain a 5 mm thick mold. Each layer was partially cured at 70 °C for 5 min (sample channel mold) or 20 min (mold for temperature control channel). The thick control layer was then peeled off from the mold and bonded to the sample-channel layer. The assembled layers were then fully cured at 70 °C for 2 h. After holes were punched, the PDMS devices were bonded onto either the cover glass or the slide glass depending on the application. In general, the devices in this study include several parallel channels: one channel for the sample and one or two channels for temperature control. The sample channel and the temperature control channels are either within the same layer or in different layers depending on required temperature gradient profiles.

Microfluidic System Operation and Particle Tracking. We used 250 nm radius carboxylate-modified polystyrene particles

(23) Ross, D.; Locascio, L. E. *Anal. Chem.* **2003**, *75*, 1218–1220.
(24) Sulabha Ranganathan, R. D. H. *Teratog. Carcinog. Mutagen.* **1989**, *9*, 29–37.
(25) Kaji, T.; Kawashima, T.; Sakamoto, M.; Kurashige, Y.; Koizumi, F. *Toxicology* **1991**, *68*, 11–20.
(26) Pittman, J. L.; Henry, C. S.; Gilman, S. D. *Anal. Chem.* **2003**, *75*, 361–370.
(27) Lucchetta, E. M.; Munson, M. S.; Ismagilov, R. F. *Lab Chip* **2006**, *6*, 185–190.
(28) Seger, U.; Panayiotou, M.; Schnydrig, S.; Jordan, M.; Renaud, P. *Electrophoresis* **2005**, *26*, 2239–2246.
(29) Hohreiter, V.; Wereley, S. T.; Olsen, M. G.; Chung, J. N. *Meas. Sci. Technol.* **2002**, *13*, 1072–1078.
(30) Park, J. S.; Choi, C. K.; Kihm, K. D. *Meas. Sci. Technol.* **2005**, *16*, 1418–1429.
(31) Unger, M. A.; Chou, H. P.; Thorsen, T.; Scherer, A.; Quake, S. R. *Science* **2000**, *288*, 113–116.

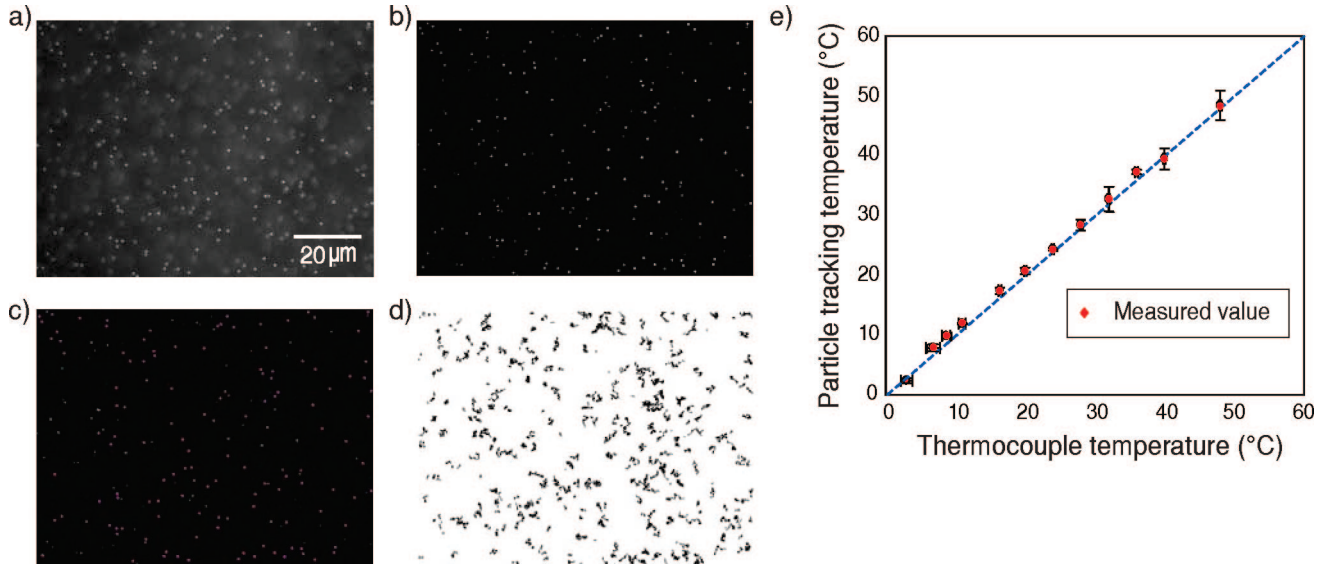

Figure 1. Tracking Brownian motion of nanoparticles correlating to temperature. (a–d) Raw and processed images of polystyrene fluorescent particles (500 ± 15 nm diameter) showing particle tracking algorithm: (a) Raw image showing in focus and out-of-focus particles. (b) Processed image by the restoring algorithm showing significantly reduced random high/low frequency noise and out-of-focus fluorescence. (c) Processed image showing the identified particle candidates (red). (d) Trajectories of the tracked particles for a duration of 49.5 s (1500 frames). (e) Comparison of temperature data from particle tracking with simultaneously measured thermocouple temperature; the dotted line representing perfect agreement between the two methods has a slope of 1.

(FluoSpheres, Invitrogen, Carlsbad, CA). Fluorescent particles were suspended in either deionized (DI) water for calibration and temperature mapping or in cell medium for in situ temperature measurements. Before every experiment, the particle suspensions were sonicated for ~30 min to break apart aggregates. After sonication the particle suspension was introduced into the particle channels, after which the in- and outlets of the particle channels were sealed with solid metal pins to eliminate fluid convection. To create temperature gradients in the devices, hot and cold fluids were first generated by flowing DI water (for the hot fluid) and 30 wt % sodium chloride solution (for the cold fluid) off-chip through temperature-controlled copper tubing and then introduced into the temperature control channels via constant pressure-driven flows. The temperature of the copper tubing was controlled using a water bath for the hot fluid and a Peltier cooler for the cold fluid. The flow rates of the hot and cold streams were set to be high enough (typically 5–10 mL/min) so that the temperature differences between inlet and outlet streams were less than 1 °C.

The Brownian motion of fluorescent nanoparticles in the particle channels was monitored via optical microscope (Leica DM-IRB) with a 63× air or 63× oil-immersion objective, and movies were captured using a CCD camera (Cohu, Poway, CA) at 30 frame/s and a resolution of 640 × 480 pixels. Subsequently the recorded movies were analyzed with software developed using Interactive Data Language (ITT Visual Information Solutions, Boulder, CO). Because Brownian motion leads to small particle displacements on these timescales and is highly sensitive to external vibrational noise, all experiments were performed on a vibration-isolated optical table. After obtaining video images from the CCD camera, we used a standard brightness-weighted centroid method to identify the particle trajectories, which involves four steps: restoring the image, locating possible particle centers, refining particle positions/eliminating unwanted particles, and linking particle positions into trajectories.[32,33] During the first step, the original image is filtered via a spatial bandpass filter to remove random high/low frequency noise. After this treatment, the image consists of bright spots on a dark background as shown in Figure 1b. The brightness-weighted centroid algorithm is then used to determine all local maxima regardless of whether they represent a real particle or not (Figure 1c). After indentifying all local maxima, cutoff criteria based on combinations of brightness and geometry were applied, such as minimum brightness and aspect ratio to remove aggregates, impurities, and out-of-focus particles. In general, aggregates have high aspect ratio and impurities have low brightness, while out-of-focus particles tend to be dimmer compared to in-focus single particles. Lastly, we connect particle positions into trajectories by comparing consecutive images (Figure 1d). These methods enable determination of the location of particles within 0.1 pixel accuracy; the conversion factor from pixel-based length scales to micrometers depends on objective magnification and CCD camera resolution.

Numerical Models for Heat Transfer. The simulations of heat transport in the devices were performed using a commercial finite element package COMSOL (Stockholm, Sweden). The convection-conduction equation was used:

$$k\nabla^2 T + \rho C_p \nu \nabla T = 0 \qquad (1)$$

where T[K] is temperature, C_p[J·kg^{-1}·K^{-1}] is the heat capacity, ρ[kg m^{-3}] is the density, ν[m s^{-1}] is the velocity vector, and k[W m^{-1} K^{-1}] is the thermal conductivity.

The actual 3-D geometries of the devices including the PDMS layers, the glass substrate, and air layer surrounding the devices were constructed. To reduce the number of mesh elements, the

(32) Crocker, J. C.; Grier, D. G. *J. Colloid Interface Sci.* **1996**, *179*, 298–310.
(33) Breedveld, V.; Pine, D. J. *J. Mater. Sci.* **2003**, *38*, 4461–4470.

thermal conductivity of the upper part of the PDMS and the actual geometry were rescaled by the equation, $k_{PDMS}/L_{PDMS} = k'_{PDMS}/L'_{PDMS}$. Heat capacities of 1100, 4180, 835, and 1006 were used for PDMS, DI water, glass, and air, respectively. Densities of 1030, 1000, 2225, and 1.205 were used for PDMS, DI water, glass, and air, respectively. Thermal conductivities of 0.17, 0.61, 1.4, and 0.025 were used for PDMS, DI water, glass, and air, respectively.[34,35]

The surface temperatures of the temperature control channels were set as an average of the inlet and outlet temperature of the fluids measured experimentally with a thermocouple (HH202A, Omega, Stamford, CT). In all experiments the temperature difference between the inlet and the outlet was found to be less than 1 °C because of the high flow rates (5−10 mL/min) and low thermal conductivity of the PDMS. The temperature of the surface of the cover glass was also set based on experimentally measured values. The temperature was kept constant by air convection from a heating fan.

Cell Culture. NIH/3T3 mouse embryonic fibroblasts (ATCC, Manassas, VA) were cultured according to standard ATCC protocols in Dulbecco's modified Eagle's medium (D-MEM with 4500 mg/L D-glucose, L-glutamine, and no sodium pyruvate, Gibco 11965, Invitrogen, Carlsbad, CA) in 5% CO_2 and 37 °C. The D-MEM was supplemented with 10% v/v bovine calf serum (HyClone, SH30073, Logan, UT) and 1% v/v antibiotic-antimycotic solution (100 IU/mL penicillin and 100 μg/mL streptomycin in 0.85% saline, Gibco 15240, Invitrogen, Carlsbad, CA). Cells were detached from their culture dish using trypsin-EDTA solution (0.05% trypsin and 0.2 g/L EDTA, Gibco 25300, Invitrogen, Carlsbad, CA). Once the cells are detached, excess D-MEM was added, and the suspension was centrifuged. The supernatant was then aspirated, and the cells were resuspended in fresh D-MEM to yield a density of ~1×10^6 cells/mL.

In Situ Temperature Measurements in the Presence of Living Cells. The experiment was performed using a PDMS microfluidic device bonded to a glass cover slip (as described earlier). To facilitate cell adhesion to the glass surface, the device was incubated with human plasma fibronectin (Gibco 33016, Invitrogen, Carlsbad, CA) in phosphate-buffered saline (PBS) at a concentration of 2 μg/mL for 30 min at room temperature. The cells were then seeded inside the device, flow was stopped, and the device was placed in an incubator (5% CO_2 and 37 °C) for 3 h to allow cell adhesion and spreading.

After incubation, the device was mounted onto the microscope stage, and images of the cells were captured (63× oil-immersion objective) to record cell morphology. The temperature was maintained at approximately 37 °C by warm air convection (heating fan) and monitored by a thermocouple attached to the surface of the cover glass adjacent to the PDMS device. A suspension of fluorescent nanoparticles (0.02% w/v in D-MEM) was then introduced into the device, and the particles were tracked (10 s movies at 30 fps) in a focal plane 25 μm above the glass surface. Tracking was performed in both fluorescent and DIC modes at two temperatures, ~37 °C and ~30 °C, as measured by the thermocouple.

(34) DOW CORNING Product Information-Sylgard 184 Silicon Elastomer.
(35) Erickson, D.; Sinton, D.; Li, D. Q. *Lab Chip* **2003**, *3*, 141–149.

RESULTS AND DISCUSSION

Brownian Motion of Nanoparticles Correlating to Temperature. The Brownian motion of nanoparticles suspended in a liquid is a result of random collisions by the constituent molecules. The random particle displacement can be quantified through the mean square displacement (MSD), a statistical measure of particle mobility that is related to diffusivity via the following equation:

$$\langle r^2 \rangle = \frac{\sum_{i=1}^{n} (\Delta x_i^2 + \Delta y_i^2 + \Delta z_i^2)}{n} = 6D\Delta\tau \quad (2)$$

where D is the diffusivity of particles and $\Delta\tau$ is the observation time interval of each incremental 3-D displacement (Δx, Δy, Δz). Equation 2 assumes that the diffusion is isotropic and that there is no convective transport. The diffusivity of particles can be described by the Stokes−Einstein equation:

$$D = \frac{d\kappa_B T}{6\pi\eta(T) r_p} \quad (3)$$

where d is dimensionality, κ_B is the Boltzmann constant, T is the absolute temperature of the fluid, r_p is the particle radius, and $\eta(T)$ is the viscosity of the fluid, which is generally a function of temperature.[30] Consequently, eqs 2 and 3 can be combined to express the MSD as a function of temperature:

$$\langle r^2 \rangle = \frac{d\kappa_B T}{\pi\eta(T) r_p}\Delta\tau \quad (4)$$

Therefore, by measuring the MSD of the suspended particle of known sizes, the surrounding liquid temperature can be easily determined.

To measure the MSD of individual nanoparticles, about 10 s of movie of suspended particles were taken at 30 frames per second, a representative frame of which is shown in Figure 1a, and processed using the modified particle tracking software (Figure 1b−d).[32] As described in the Experimental Method and Materials section, the software applies four analysis routines: restoring images (Figure 1b), locating possible particle candidates (Figure 1c), eliminating unwanted particles, and linking the time-resolved locations into trajectories (Figure 1d) to calculate the MSD.

We measured the MSD of the nanoparticles for temperature ranging from 1 to 50 °C. The calculated temperature shows excellent agreement with the corresponding temperature measured by a thermocouple (Figure 1e), which is consistent with previously published data.[29,30] As shown in Figure 1e, when using 500 nm (±15 nm) particles, this method provides an overall accuracy of temperature measurement of less than 1 °C.

The advantage of temperature measurements using the MSD is that the accuracy is not affected by spatial variations in excitation illumination and detection efficiency. The reason is that, as described in the Experimental Method and Materials section, particle tracking microscopy uses intensity contrast between particles and local background to locate the center of particles and does not rely on quantitative analysis of fluorescence intensity, thus avoiding problems associated with photobleaching. More-

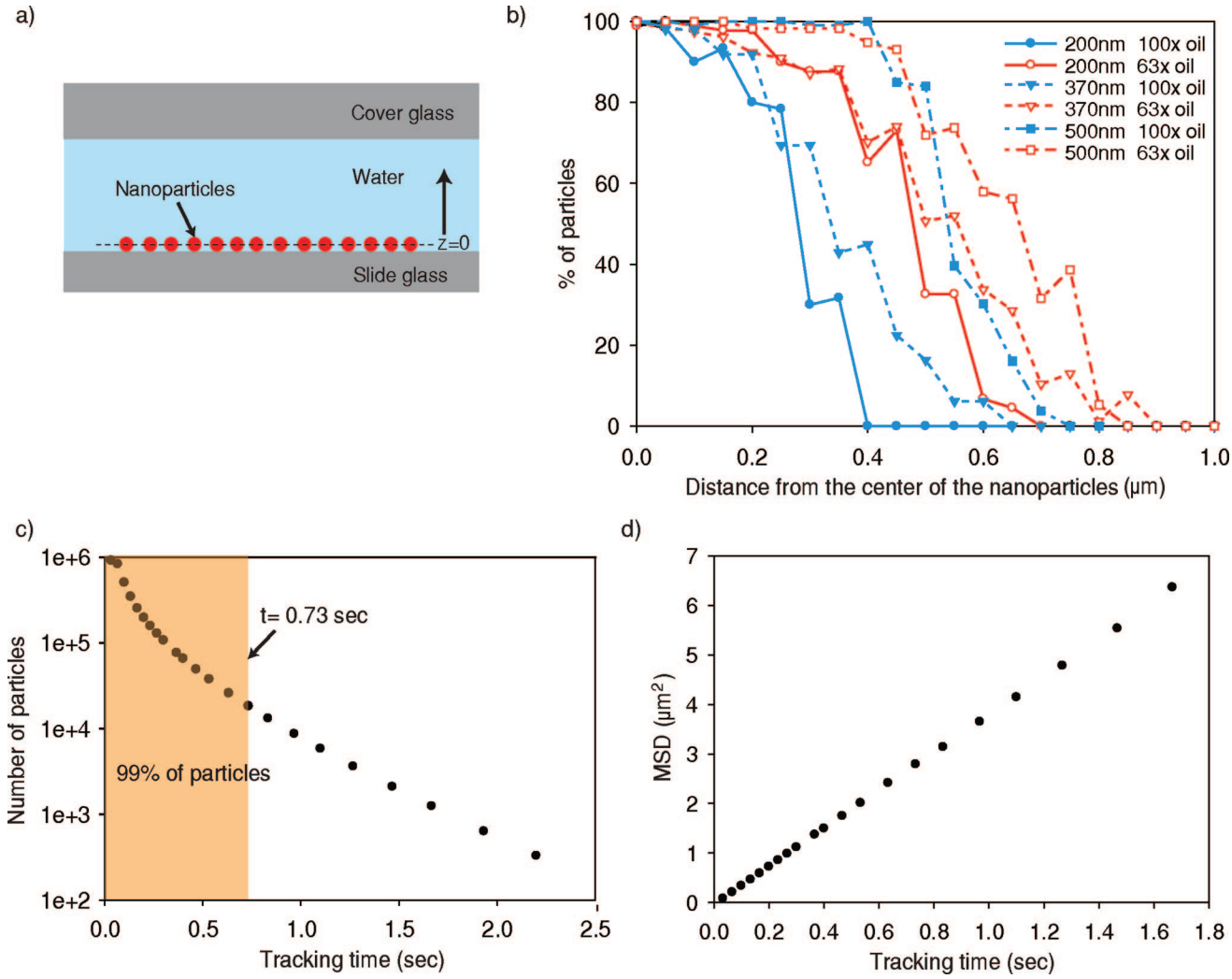

Figure 2. Mechanism of 3-D temperature mapping using Brownian motion of nanoparticles. (a) Schematic of a sample slide for determining spatial resolution in the axial dimension. (b) Percentage of particles identified by the software algorithm as a function of distance from the center of particles. *Z*-stacks with a 50 nm step size were acquired and processed. (c) The distribution of tracking time of the particles in the case when 500 nm diameter particles were imaged with 63× air objective. (d) Corresponding MSD of the 500 nm particles as a function of the tracking time at 25 °C.

over, the methodology is not limited to the fluorescence mode; it can equally well be used for images obtained in the differential interference contrast (DIC) mode. The calibration experiments thus show that this method provides accurate absolute temperature measurements with excellent robustness, independent of experimental conditions.

Mechanism of 3-D Temperature Mapping. Previously Benninger et al. described a spectroscopic method using temperature sensitive chemicals to map 3-D temperature profiles.[20] Although elegant, this method requires a multiphoton optical sectioning setup to provide 3-D data stacks and also to eliminate out-of-plane fluorescence that could skew the observed temperature distributions. While this method offers high resolution and accuracy, microscopes with the multiphoton optical sectioning setup are at least an order of magnitude more expensive than conventional microscopes. In contrast, we provide a method for 3-D temperature mapping with a simple and inexpensive video-microscopy setup. This can be achieved by using the software algorithm that distinguishes in-focus particles in a dense particle suspension despite the presence of significant out-of-focus fluorescence. By selectively tracking the in-focus particles, the temperature of a focal plane can be measured. Therefore, 3-D temperature maps can be obtained by measuring temperature from a series of images at different focal planes.

In this method, the vertical resolution of each temperature measurement depends upon the tracking depth, which is defined as the distance above and below the measurement focal plane, outside of which particles cannot be tracked by the software algorithm. The tracking depth depends on particle size and microscope optics. To experimentally determine the tracking depth, a sample specimen with a single layer of particles was prepared (Figure 2a), and a series of images at different focal planes with a 50 nm step size were acquired from the center ($z = 0$ in Figure 2a) of particles in the vertical direction. Figure 2b shows the percentage of particles the algorithm can identify as a function of vertical distance above the particle layer. For example, with 200 nm particles and a 100× oil objective, the tracking depth is found to be 0.4 μm above and below the focal plane, which corresponds to a minimum vertical measurement resolution of 0.8 μm.

The small tracking depth not only enables temperature measurement in the vertical direction but also allows two-

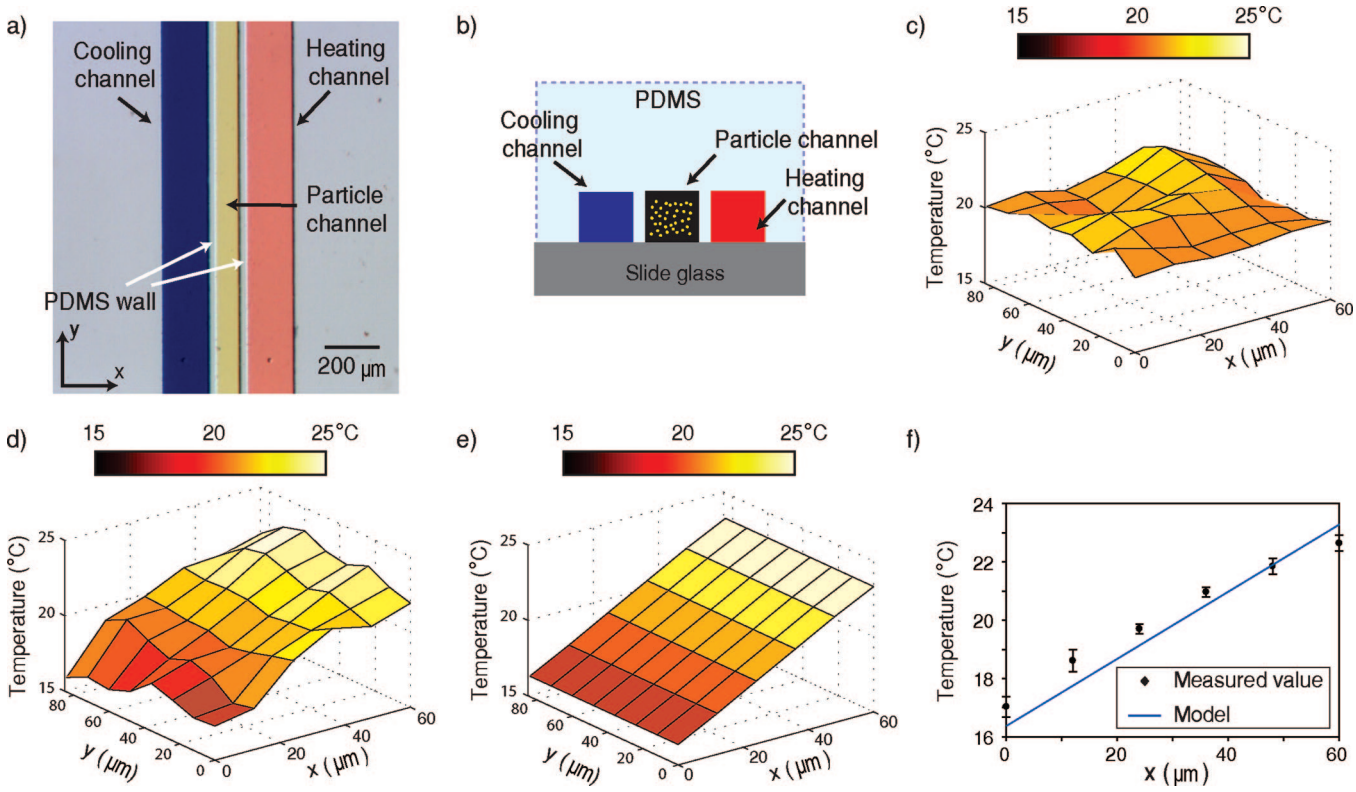

Figure 3. 2-D temperature mapping. (a) Optical micrograph of the microdevice fabricated using soft lithography. The temperature control channels colored with red (hot stream) and blue (cold stream) were 200 μm × 80 μm (width × height), and the tracer particle loading channel colored with yellow was 60 μm × 80 μm (width × height). The temperature distribution in the detection zone was generated by flowing two streams with controlled temperatures through the temperature control channels. (b) Schematic of cross-sectional view. (c, d) False-color images of measured temperature distribution: (c) with no imposed temperature gradient at room temperature, and (d) in the presence of temperature gradient. Hot stream, ~35 °C; cold stream, ~5 °C. (e) Corresponding numerical simulation. (f) Horizontal temperature line profile at height of 40 μm across the particle loading channel. Black circles, measured values; blue line, numerical prediction.

dimensional (2-D, *x* and *y*) temperature mapping in a focal plane. This is possible because the 3-D random motions of nanoparticles cause them to move in and out of the tracking range, thereby limiting the length of time during which each particle can be tracked. The MSD value associated with the trajectory of the particle can be assigned to the location of the center of mass of the tractory. In this scenario, the MSD value associated with the trajectory corresponds to the *x* and *y* resolution of the measurement. As an example, using 500 nm particles with a 63× air objective (Figure 2c), the tracking time of 99% of particles was less than 0.7 s at room temperature. The corresponding MSD of the particles was less than 3 μm^2 (Figure 2d). Therefore, the temperature calculated from each MSD represents a local value defined by the distance explored by the particle, 1.7 μm. These results show that the spatial resolution of our simple videomicroscopy method is as low as 1~2 μm in all dimensions. Therefore, 3-D temperature mapping can be achieved without using multiphoton optical scanning.

2-D Temperature Mapping. In some microfluidic applications, spatial temperature gradients in a microscale channel are desired to study temperature-sensitive biological phenomena, such as the rate of cell division.[7] To demonstrate the capability of our method to measure spatial variations of temperature in such systems, we performed temperature measurements in a microfluidic device that was specifically designed to generate a temperature gradient. Two parallel temperature control channels (Figure 3a,b) sandwich a middle channel that is filled with particle suspension. We first measured the temperature distribution at room temperature with no imposed temperature gradient. Figure 3c shows a false-color image of measured temperature distribution. The standard deviation of temperature is 0.62 °C, which is small and gives an indication of the temperature resolution one can get with our technique.

We then created a temperature gradient across the particle filled channel by flowing a cold stream of ~5 °C and a hot stream of ~35 °C through the parallel side channels (Figure 3a,b). Figure 3d illustrates the measured temperature distribution in the presence of a temperature gradient, with Figure 3e showing the results of the corresponding numerical simulation. As expected, both the experimental data and the numerical simulation demonstrate that temperature increases as a linear function of distance from the cooling side to the heating side with a rise in fluid temperature of ~ 6 °C. This temperature gradient is quantified in Figure 3f, for which the horizontal (*x*-direction) temperature profile at height of 40 μm (center of the channel in the *z*-direction) was read. The observed temperature gradient corresponds well with the numerical simulation, typically within 1 °C. Discrepancies between the predicted temperature and the measured temperature are in part due to slight geometric inconsistencies between the actual microfabricated channels and the one used in the numerical simulation. In addition, during operation of the device, we observed that flowing pressurized streams slightly deformed the thin PDMS wall between the heating/cooling channels and the particle loading channel, which was not taken into account in

the numerical simulation. Additionally, uncertainties in the thermal properties of PDMS and the surrounding boundary temperatures may contribute to the discrepancies.[35,36]

In these experiments, we demonstrated that tracking individual particles enables spatially resolved temperature measurement in the horizontal direction with a resolution of ~12 μm. We note that, although the theoretical optical resolution for our 63× objective is less than 2 μm, to reduce experimental uncertainty we needed to discretize the field of view as shown Figure 3c−e so that each domain contains more trajectories of particles to increase the number of data points. This resolution can be easily improved by using higher magnification objectives, higher speed cameras, particle suspensions of higher concentration, and/or 3-D particle tracking.[30]

3-D Temperature Mapping. Many microfluidic systems are multifunctional and highly integrated. This functional requirement results in increased complexity of microchannel networks and often requires 3-D layering of the components.[5,28] For example, microfabricated electrodes for DEP are normally fabricated on a dielectric substrate (such as glass), and Joule heating caused by the operation of electrodes could generate temperature gradients along the horizontal and the vertical direction inside the channel.[28] To demonstrate the potential application of our thermometric method in the vertical direction (z-axis), we measured the temperature distribution in a multilayered microfluidic device that generates a temperature gradient perpendicular to the glass substrate. Panels a and b of Figure 4 illustrate the geometry of the multilayer PDMS device. The temperature gradient was created by flowing coolant at −8 °C through the temperature control channel in the top layer. Air-filled channels were placed parallel to the particle loaded channel for insulation to minimize temperature gradients in the horizontal direction. The surface temperature of the cover glass was controlled by warm air from a heating fan and measured to be 30 °C. We obtained a z-stack of movies of nanoparticles with a step size of 12 μm and processed these movies with the image analysis algorithm to achieve optical sectioning.

Figure 4c shows the experimentally measured and numerically predicted temperature profiles in the channel as a function of z, the height above the glass surface. The observed temperature variation was consistent with the numerical modeling. Although the PDMS membrane between the coolant channel and the particle channel is relatively thin (~40 μm) compared to the height of the channel and the thickness of the coverglass, a large temperature increase of ~12 °C occurred in the membrane as expected because of the inherently low thermal conductivity of PDMS (0.17 W/mK). Because polymeric materials including PDMS have been broadly used for devices that control temperature in microchannels,[5,37] the low thermal conductivity of the polymeric materials must be taken into account in device design.

In Situ Temperature Measurements in the Presence of Living Cells. In situ temperature measurements via nanoparticle tracking were performed in the presence of living cells to test the robustness and compatibility of the measurement method in biological experiments. NIH/3T3 fibroblasts were seeded onto the glass surface inside a microchannel in a PDMS device that

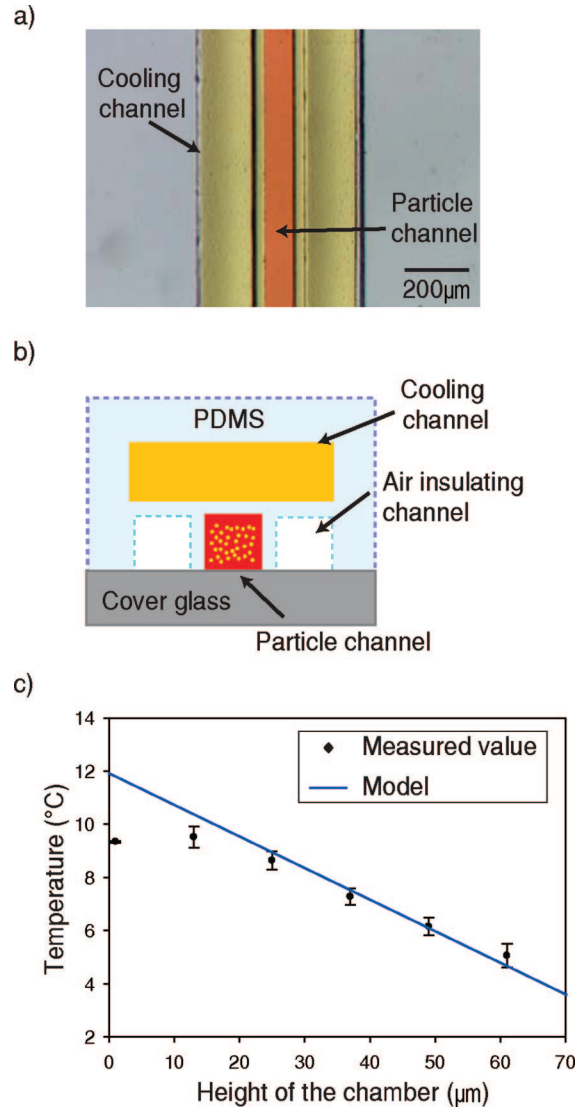

Figure 4. 3-D temperature mapping. (a) Optical micrograph of the microdevice fabricated using multilayer soft lithography: yellow, temperature control channel; red, particle loading channel. (b) Schematic of cross-sectional view. (c) Comparison between experimentally measured and numerically predicted temperature profiles as a function of height in the particle loading channel showing good agreement. Black circles, measured values; the blue line, numerical prediction.

was pre-incubated with 2 μg/mL fibronectin. A 0.02% w/v suspension of nanoparticles in D-MEM was introduced into the device, and the MSD of the particles was measured in two different microscopy modes (fluorescence and DIC) at two temperatures. MSD measurements (representative images shown in Figure 5) and measured viscosity data of D-MEM (data not shown) were then used to calculate the corresponding temperatures on chip.

Temperatures calculated from in situ MSD measurements agreed well with those reported by the thermocouple, demonstrating the ability of the in situ method to function in the presence of adherent cells. Under heated conditions (from the heating fan), in situ measurements yielded a temperature of 37.9 ± 0.8 °C, and 36.7 ± 1.9 °C in fluorescent and DIC modes, respectively (see Figure 5). The thermocouple, placed on the surface of the glass substrate outside the PDMS device, measured 39.0 °C. At a lower temperature, the in situ measurements yielded temperatures of

(36) McDonald, J. C.; Whitesides, G. M. *Acc. Chem. Res.* **2002**, *35*, 491–499.
(37) Mao, H. B.; Yang, T. L.; Cremer, P. S. *J. Am. Chem. Soc.* **2002**, *124*, 4432–4435.

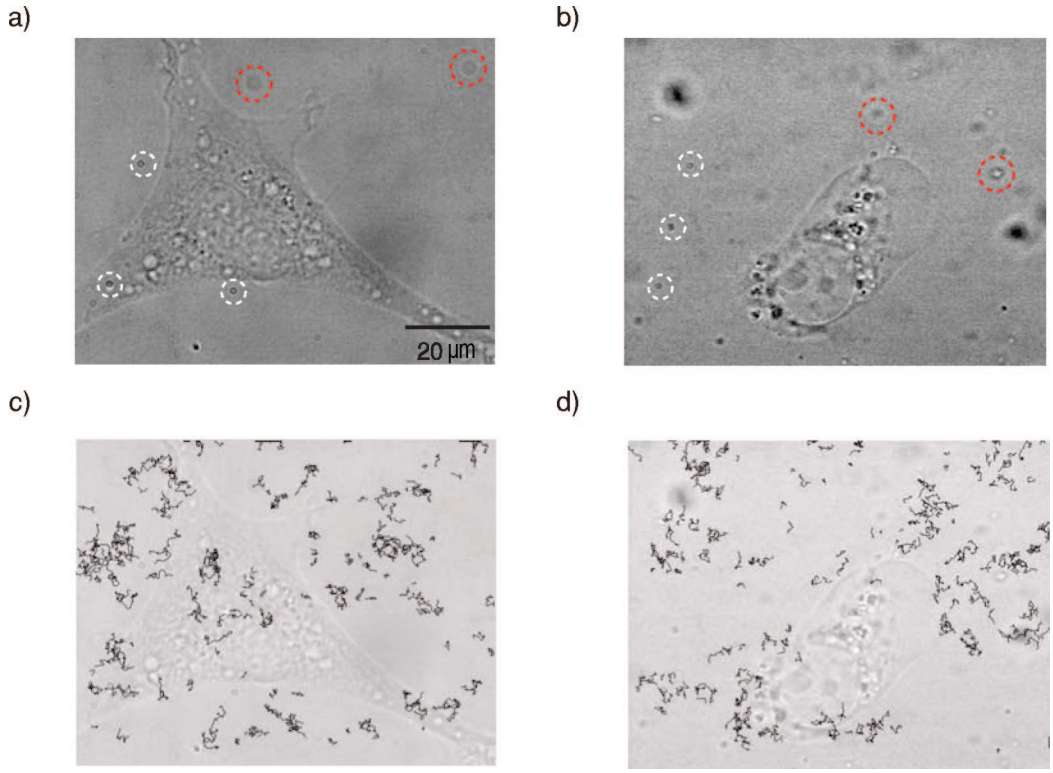

Figure 5. In situ temperature measurement in the presence of biological samples. (a, b) Images in DIC mode, showing a NIH/3T3 cell and tracer particles in the chip. Focal plane of measurement is located 15 μm above the glass surface; white circles indicate representative particles in the focal plane while red circles indicate representative particles out of the focal plane. Temperature of the chip was controlled by convection (heating fan), and near-cell temperature was measured using the presented method in both fluorescent mode and DIC mode. (a) At ~37 °C (Fluorescent mode: 37.93 ± 0.77 °C, DIC mode: 36.70 ± 1.86 °C). (b) At ~29 °C (Fluorescent mode: 29.12 ± 0.84 °C, DIC mode: 29.68 ± 0.99 °C). The fully spread morphology at ~37 °C (pointed, triangular) changes to a contracted morphology at ~29 °C, which is expected of this adherent cell line. (c, d) Overlay of the cell images of (a,b) and the processed images showing trajectories of particles at ~29 °C in (c) fluorescent mode and (d) DIC mode.

29.1 ± 0.8 °C and 29.7 ± 1.0 °C, in fluorescence and DIC modes, respectively. In that case, the thermocouple read a temperature of 28.5 °C. The differences between the in situ and thermocouple measurements can be attributed to the location of the thermocouple relative to the microchannel and the direction of convective heating from the fan. Since the heating fan was blowing down from above the device, the thermocouple was directly exposed to the air current, while the microchannel was shielded by the 5 mm-thick PDMS layer and faced the cooler underside of the device. Therefore, a slightly higher temperature at the thermocouple is expected under heated conditions.

The introduction of nanoparticles into the medium surrounding cells did not cause an observable change in cell morphology for at least 3 h. This observation suggests that the nanoparticles do not affect cell viability, at least in the short term. Since in situ temperature measurements can be performed in as little as 10 s, it is very easy and practical to introduce the particles, perform experiments, and replace the medium to remove the particles before the particles interact with cells. An advantage of the in situ measurement technique shown here is that it works not only in fluorescence but also in a transmitted light mode (DIC, in this case). Cellular features and outlines can be seen in the background of each image when operating with transmitted light, but such background images did not interfere with MSD measurements (Figure 5c,d). This feature makes it possible to monitor cells while tracking the temperature, which opens new possibilities to study temperature-dependent cell responses, such as morphological changes in cell injury induced by temperature shifts,[38,39] immunological response of cells after local hyperthermia,[40] and cell signaling under cold stresses.[41] In addition, the transmitted light mode does not suffer from potential photobleaching, which makes the technique more widely applicable.

CONCLUSIONS

In this work, we have demonstrated for the first time that tracking Brownian motion of nanoparticles can be used for 3-D in situ thermometry in microfluidic devices. In contrast to fluorescence intensity measurement techniques, particle tracking is independent of fluorescent intensity. In particular, the use this methodology in combination with DIC mode microscopy completely eliminates photobleaching-related problems. Thus, this method offers accurate temperature measurements with superior reproducibility and reduced systematic error. Another notable advantage of this method is that it provides 3-D temperature mapping without using an expensive multiple-

(38) Liepins, A.; Bustamante, J. O. *Scanning Microsc.* **1994**, *8*, 631–643.
(39) Davidson, J. F.; Whyte, B.; Bissinger, P. H.; Schiestl, R. H. *Proc. Natl. Acad. Sci. U.S.A.* **1996**, *93*, 5116–5121.
(40) Kubes, J.; Svoboda, J.; Rosina, J.; Starec, M.; Fiserova, A. *Physiol. Res.* **2008**, *57*, 459–465.
(41) Zhu, J. K. *Curr. Opin. Plant Biol.* **2001**, *4*, 401–406.

photon scanning setup. The use of a software algorithm and the associated small tracking depth offer a spatial resolution up to 1−2 μm in the vertical direction. The most unique advantage of this method over conventional methods is that this method can be used for in situ temperature monitoring. We also note that one potential drawback of our method is that fluid must be stopped to track accurately Brownian motion of particles. However, recent developments in particle tracking technology have shown that Brownian motion of particles is measurable in the presence of convection flow. Implementation of these more advanced particle tracking algorithms will not only enable temperature measurement in convection flow but also broadens its application to the simultaneous measurement of fluid temperature and velocity distributions.

ACKNOWLEDGMENT

The first two authors contributed equally to this work. The authors acknowledge the National Science Foundation (DBI-0649833 to HL, CTS-0547066 to VB) for funding, and J. Stirman, M. Crane, A. Hirsch, and L. Cheplen for technical assistance.

Received for review September 24, 2008. Accepted December 9, 2008.

AC802031J